

Chemical Modification and Organelle-Specific Localization of Orlistat-Like Natural-Product-Based Probes

Peng-Yu Yang,^[a] Kai Liu,^[b] Chongjing Zhang,^[a] Grace Y. J. Chen,^[a, b] Yuan Shen,^[a] Mun Hong Ngai,^[a] Martin J. Lear,^[a] and Shao Q. Yao^{*,[a, b]}

On the occasion of the 10th anniversary of click chemistry

Abstract: Orlistat, also known as tetrahydrolipstatin (THL), is an FDA-approved anti-obesity drug with potential anti-cancer activity. Previously, we developed a chemical proteomic approach, based on the Orlistat-like probe (**1a**) for large-scale identification of unknown cellular targets of Orlistat in human hepatocytes. In this article, we report the chemical synthesis and biological evaluation of an expanded set of Orlistat-like compounds, with the intention to further dissect and manipulate potential cellular targets of Orlistat. In doing so, we carried out proteome-wide activity-based profiling and

large-scale pull-down/LCMS analysis of these compounds in live HepG2 cells, and successfully identified many putative cellular targets for Orlistat and its structural analogues. By qualitatively assessing the spectra counts of potential protein hits against each of the seventeen Orlistat analogues, we obtained both common and unique targets of these probes. Our results revealed that

subtle structural modifications of Orlistat led to noticeable changes in both the cellular potency and target profiles of the drug. In order to further improve the cellular activity of Orlistat, we successfully applied the well-established AGT/SNAP-tag technology to our cell-permeable, benzylguanine (BG)-containing Orlistat variant (**4**). We showed that the drug could be delivered and effectively retained in different sub-cellular organelles of living cells. This strategy may provide a general and highly effective chemical tool for the potential sub-cellular targeting of small molecule drugs.

Keywords: chemical proteomics · click chemistry · orlistat · SNAP-tag technology · structure–activity relationships

Introduction

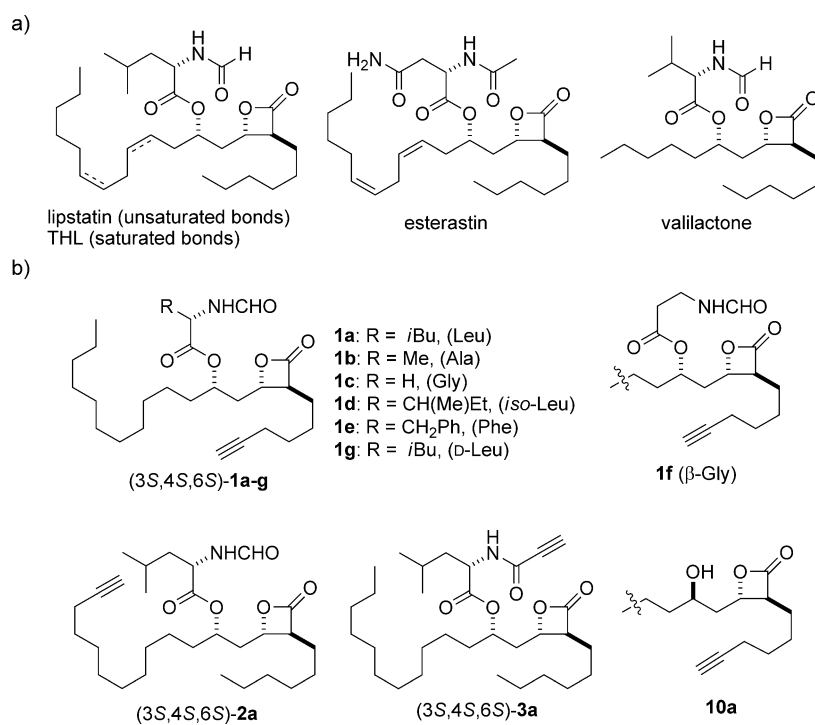
Accurate and thorough determination of drug–target interactions is of great importance in drug discovery. It offers invaluable biological insights for a drug candidate, such as its mode of action both *in vitro* and *in vivo*, and also provides clues for compound optimization in order to maximize the

therapeutic potential and minimize the potential cellular toxicity of a drug.^[1] Recent advances in chemical proteomics, a multidisciplinary research area integrating biochemistry and cell biology with organic synthesis and mass spectrometry, have enabled a more-direct and unbiased analysis of a drug's mechanism of action in the context of the proteomes as expressed in the target cell or the tissue of interest.^[2] However, at present, few methods are available for the large-scale profiling of drug–protein interactions *in vivo*.^[3] We recently reported a chemical proteomic method that makes use of natural-product-like small-molecule probes for proteome-wide profiling of putative drug targets in living cells.^[4] That strategy is based on the concept of activity-based protein profiling (ABPP), originally coined by the Cravatt group and further developed by other groups.^[3,5,6] In our studies, terminal-alkyne-containing probes based on Orlistat or tetrahydrolipstatin (THL, Scheme 1), an FDA-approved anti-obesity drug, were developed.^[7]

[a] P.-Y. Yang, C. Zhang, G. Y. J. Chen, Y. Shen, M. H. Ngai, Prof. Dr. M. J. Lear, Prof. Dr. S. Q. Yao
Department of Chemistry
National University of Singapore
3 Science Drive 3, Singapore 117543 (Singapore)
Fax: (+65) 6779-1691
E-mail: chmyaosq@nus.edu.sg

[b] K. Liu, G. Y. J. Chen, Prof. Dr. S. Q. Yao
Department of Biological Sciences
National University of Singapore
14 Science Drive 4, Singapore 117543 (Singapore)

Supporting information for this article is available on the WWW under <http://dx.doi.org/10.1002/asia.201100306>.



Scheme 1. a) Representative structures of the lipstatin family of natural products possessing *trans*-3,4-disubstituted- β -lactones. b) Previously published Orlistat-like probes (**1a–1g**, **2a**, and **3a**) and the key intermediate **10a**.^[4a,c]

Orlistat works primarily on pancreatic and gastric lipases within the gastrointestinal (GI) tract.^[7] Recently, Orlistat and other lipstatin-based natural products have shown promising anti-tumor activities by potently inhibiting human fatty acid synthase (FAS) in tumor cells.^[8] FAS is an enzyme essential for the survival of cancer cells.

In our approach, extremely conservative modifications (i.e., an alkyne handle; see **1a** in Scheme 1) were introduced in the parental Orlistat structure to provide the necessary functionality for target identification via copper(I)-catalyzed 1,3-dipolar cycloaddition (click chemistry) or copper catalyzed azide–alkyne cycloadditions (CuAAC),^[9] whilst maintaining the native biological properties of the drug. When combined with affinity purification and LCMS analysis, we were able to identify and putatively validate several previously unknown cellular targets of Orlistat, including GAPDH, β -tubulin, Annexin A2, Hsp90AB1 and three ribosomal proteins (RPL7a, RPL14, and RPS9).^[4a] Although some of these are highly expressed endogenously, and their presence might be explained primarily by their relative cellular abundance, such information is important to better understand the full biological effects of a drug.

Having said this, there are still a number of challenges that prevent Orlistat from being considered as a potential anti-tumor drug; it has poor solubility and bioavailability, and, most importantly, it lacks sufficient potency and specificity. To begin to address some of these issues, we and others previously focused on the development of highly efficient chemistry which has enabled the facile synthesis of Or-

listat analogues by performing various chemical modifications on the aliphatic side-chains around the β -lactone core of the drug.^[4b,10] In our preliminary studies using different Orlistat-like compounds, we found a direct link between the chemical modification of Orlistat and its cellular activity.^[4b] However, no further studies were carried out to explain the potential cellular targets of these analogues and their biological consequences. Another way to achieve good in vivo efficacy of bioactive compounds is to deliver them into the sub-cellular compartment of cells where the target enzyme resides. In this way, an increase in the effective concentration of the inhibitor (i.e. improved potency) with a better selectivity would be expected. In fact, such sub-cellular targeting has recently been demonstrated successfully for several inhibitors and small-

molecule probes in cultured cells.^[11] Herein, we report further chemical and cellular modifications of Orlistat with the ultimate aim to improve its cellular activities (Figure 1 and Scheme 3). By using an expanded set of new Orlistat-like probes, we performed in situ proteome-profiling experiments following treatment of live HepG2 cells with our probes (Figure 1). Large-scale pull-down/LCMS identifications of potential cellular targets were subsequently conducted. From these studies, both common and unique protein targets of Orlistat-like analogues were identified. In order to further improve Orlistat's cellular activities, we developed a "cellular modification" strategy to deliver our cell-permeable Orlistat variant to different sub-cellular organelles in living cells (Scheme 3). This strategy was successfully implemented by taking advantage of the well-established AGT/SNAP-tag technology.^[12]

Results and Discussion

Design and Synthesis of Orlistat-Like Probes

The design of Orlistat-like probes was based on the general structure of a number of naturally occurring congeners of lipstatin (namely lipstatin, esterastin, and valilactone; Scheme 1 a), and our previously reported compounds, **1a–g**, **2a**, and **3a** (Scheme 1 b),^[4a,c] in which a terminal C–C single bond in one of the aliphatic chains in the parental Orlistat structure was substituted for a C–C triple bond. This extremely conservative modification was previously shown to

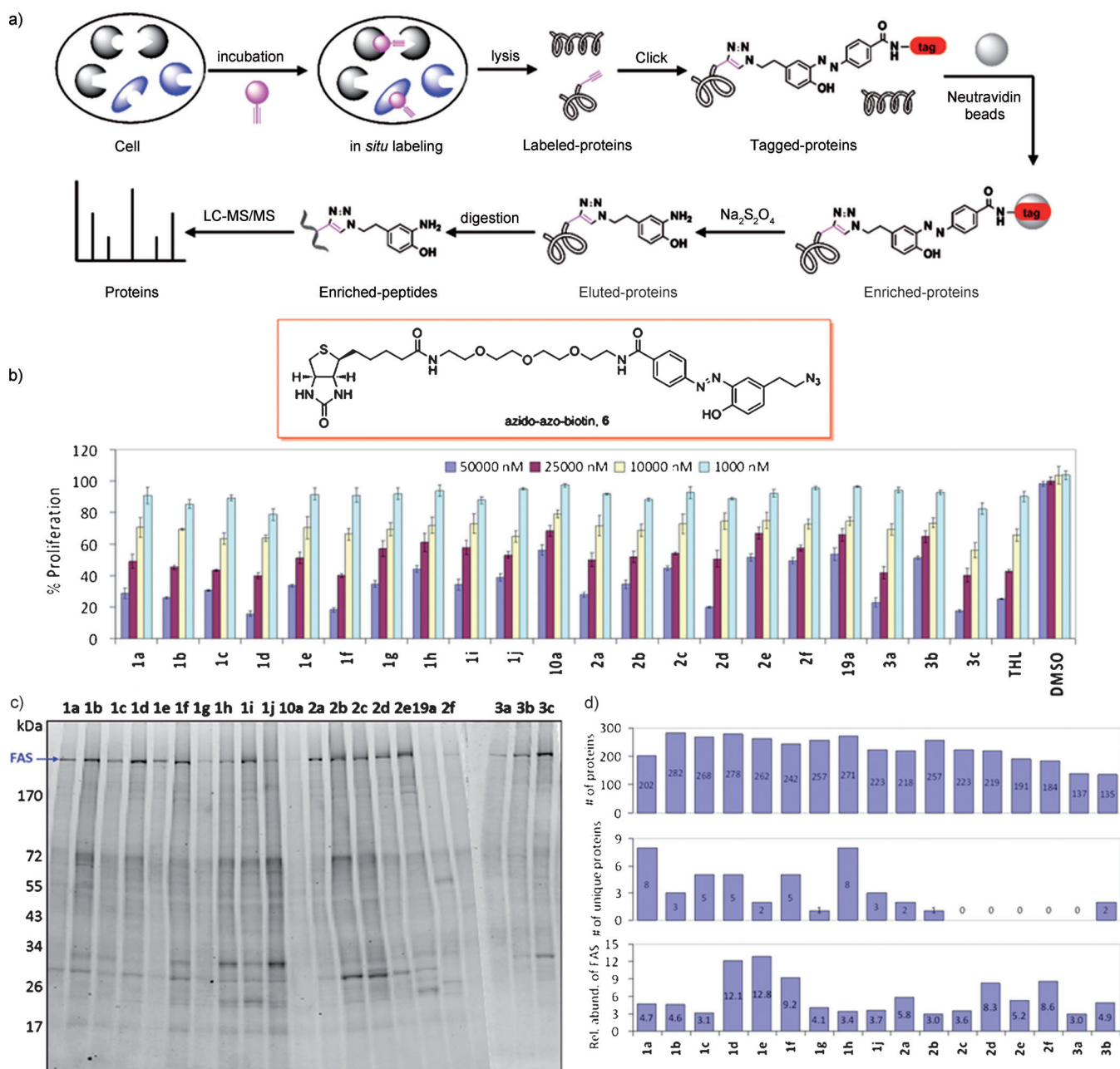
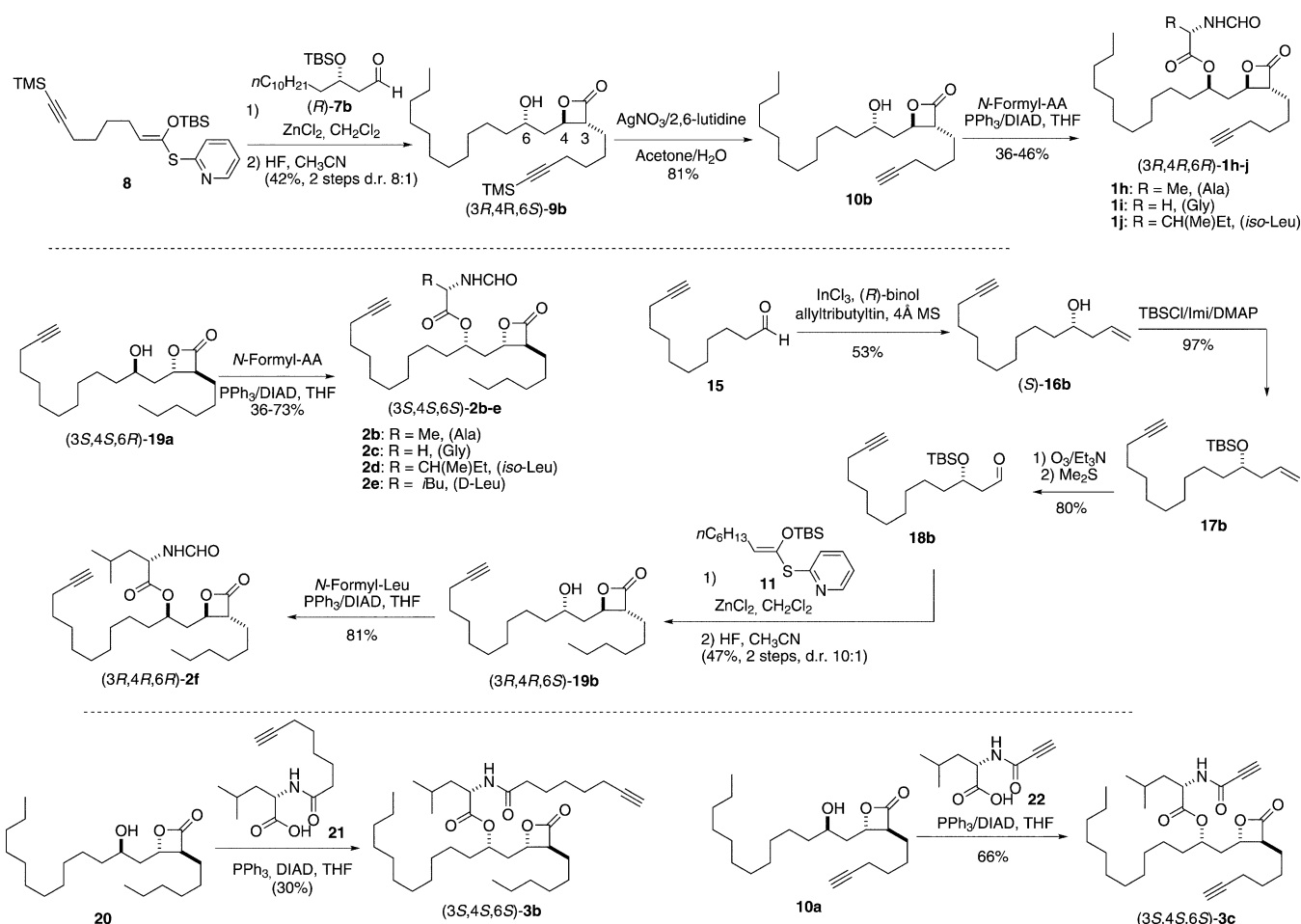


Figure 1. Biological screening of Orlistat-like compounds in live HepG2 cells. a) Overall workflow of the large-scale affinity pull-down/LC-MS/MS experiments. The chemically cleavable linker, **6**, used in study is shown in red. b) Dose-dependent inhibition of HepG2 cell-proliferation by the 21-member Orlistat library using an XTT assay. The data represent the average standard deviation for two trials. Wild-type Orlistat (positive control) and DMSO (negative control) were included in the assay. c) In situ proteome-profiling of Orlistat analogues against HepG2 cells. Probe-labeled proteins were detected by click-chemistry-mediated coupling to a rhodamine-azide reporter tag, followed by SDS-PAGE and in-gel fluorescence scanning. The arrow indicates the labeled FAS band. d) Summary of proteins identified in all seventeen Orlistat-like compounds. Top: total number of proteins identified from each probe; Center: total number of unique proteins identified from each probe; Bottom: relative percentage abundance of FAS (calculated from the emPAI value for FAS in the experimental sample/the sum of the emPAI values for FAS in all seventeen samples) obtained from each probe.

enable full retention of the native biological activities of Orlistat, and at the same time allow for subsequent chemical profiling/target identification by the downstream conjugation of reporter tags by bio-orthogonal click chemistry.^[4a] We now report the synthesis, anti-proliferation evaluation, and proteomic-profiling results of an expanded list of Orlistat analogues that incorporate various degrees of molecular

complexity (i.e. changes in the position of the terminal-alkyne handle, the amino ester, and in the chirality; Scheme 2). This detailed investigation has refined our present understanding of the anti-proliferative role played by Orlistat and has established certain structure-activity relationships (SARs) within this drug's structural motif from which the next generation of designed analogues may



Scheme 2. Synthesis of probes **1h–j**, **2b–f**, and **3b–c** used in this study. THF = tetrahydrofuran, DIAD = diisopropyl azodicarboxylate, binol = 1,1'-binaphthalene-2,2'-diol, Imi = imidazole, DMAP = 4-dimethylaminopyridine.

emerge. To this end, ten new analogues of Orlistat were synthesized (Scheme 2). In the analogue series **1h–j**, the left-hand aliphatic side-chain remained intact, whilst the nature of the amino ester and/or the chirality at the C3, C4, and C6 positions were varied strategically. In the analogue series **2b–f**, the right-hand aliphatic side-chain was kept constant, whilst the structure of the amino ester (**2b–e**) and the chirality at the C3, C4, and C6 positions (**2f**, containing an *N*-formyl-L-leucine moiety) were altered. For the analogue **3b**, further structural changes were made at the *N*-formyl group by the introduction of a long alkyne-containing acyl group. In the case of **3c**, the two terminal alkyne handles were simultaneously introduced (top and right).

As shown in Scheme 2, the synthesis of Orlistat analogues **1h–j** began with the previously prepared enantiopure aldehyde **7b** from commercially available dodecan-1-ol.^[4a] This synthetic sequence, which relied on the kinetic resolution of racemic allylic alcohols, was chosen because of its applicability to large-scale synthesis and convenient variation of the chirality at the C3, C4, and C6 positions. Briefly, aldehyde **7b** was treated with thiopyridyl ketene acetal **8** under standard tandem Mukaiyama-aldol/lactonization (TMAL) reac-

tion conditions,^[10] thus providing the silyloxy- β -lactone intermediates as a mixture of diastereomers (ca. 8:1 *anti/syn*) with complete selectivity for the *trans*- β -lactones. Subsequently, direct O-desilylation allowed the isolation of the enantiomerically pure γ -hydroxyl β -lactones **9b**. Subsequent C-desilylation with AgNO₃/2,6-lutidine gave the terminal acetylene **10b**, which was subjected to Mitsunobu conditions with various *N*-formyl amino acids, thus giving rise to the corresponding configurationally inverted products **1h–j**. Similar to **2a**, compound **2b–e** were conveniently synthesized from key intermediate **19a** with various *N*-formylated amino acids under Mitsunobu conditions, thereby giving rise to the corresponding configurationally inverted products in a single step. The synthesis of **2f** commenced with the optically active aldehyde **16b**, which was obtained by enantiomeric enrichment using an asymmetric allylation (allyltributyltin/binol/InCl₃) reaction.^[13] Following *tert*-butyldimethylsilyl (TBS) protection and oxidative cleavage, the desired aldehyde **18b** was obtained, which, following further TMAL and Mitsunobu reactions, led to the desired Orlistat analogues **2f**. For the synthesis of **3b**, the known hydroxyl- β -lactone **20** was first prepared as previously described.^[4a] Sub-

sequent treatments with **20** and **21** under Mitsunobu conditions furnished the targeted analogue **3b**. Compound **3c** was conveniently synthesized from the key intermediate **10a** with **22** under Mitsunobu conditions.

Biological Screening and In Situ Proteome Profiling of Orlistat Analogues

With these ten new Orlistat analogues in hand (**1h–1j**, **2b–2f**, **3b–3c**), together with the wild-type Orlistat, the nine previously reported Orlistat analogues (**1a–1g**, **2a**, **3a**) and two key intermediates (**10a** and **19a**), a total of twenty-two compounds were tested for their anti-proliferative activities against the human liver cancer line HepG2 using the XTT assay described previously,^[4a–b] followed by in situ proteome profiling and target identification using affinity pull-down/LCMS approaches (Figure 1). The overall workflow of the strategy is shown in Figure 1a.

As shown in Figure 1b, nine of the compounds examined (**1a–1c**, **1d**, **1f**, **2a**, **2d**, **3a** and **3c**) displayed comparable activities to Orlistat in blocking the proliferation of HepG2 cancer cells. A closer examination of the data revealed a noteworthy structure–activity relationship (SAR) between the compounds tested and their anti-proliferative activities. In general, the chirality of the Orlistat analogues is important for activity. For example, in a direct head-to-head comparison, compounds with an inverted stereochemistry at the C3, C4 and C6 positions (*S* to *R*), i.e., **1b–d** versus **1h–j**, and **2a** versus **2f**, were shown to have significantly lower anti-proliferative activities. The stereochemistry of the α -carbon position in the *N*-formylated amino ester moiety of Orlistat also had a notable effect on its activity: both **1a** and **2a** (which are structurally identical to Orlistat, except with a switch in the position of the $C\equiv C$ group between aliphatic chains) appeared to be more active than their corresponding epimers, **1g**, and **2e**, respectively. The *N*-formylated amino ester moiety as a whole appeared to be essential for anti-proliferative activity, as demonstrated by the lack of activity in the two hydroxyl lactone intermediates, **10a** and **19a** (in which the *N*-formylated amino ester was completely deleted). It should be noted that, in a previous study, the *N*-formyl group of Orlistat had also been shown to be highly sensitive to the inhibition of FAS.^[10b] The different anti-proliferative profiles displayed by Orlistat-like compounds have likely been accumulated through their inhibition against a multitude of cellular targets, including FAS, in HepG2 cells. Indeed, many drugs appear to work by synergistically targeting multiple proteins.^[14]

In situ Proteome Profiling and Target Identification

We then carried out in situ proteome-reactivity profiles of all probes to identify potential cellular targets which were covalently labeled by the probes in live HepG2 cells. Following previously published procedures with some modifications (summarized in Figure 1a),^[4a] each probe (20 μ M) was added directly to the cell culture medium. After two hours

of incubation, the cells were washed (to remove excess probes), homogenized, incubated with rhodamine–azide (for the structure, see the Supporting Information, Figure S1) under click chemistry conditions, separated by SDS-PAGE gel, and analyzed by in-gel fluorescence scanning. As shown in Figure 1c, FAS in general was the main cellular target of these probes in HepG2 cells, as evident from the in-gel fluorescence scanning in which it showed up as the most strongly labeled band amongst all of the labeled bands. This profile is similar to the labeling profiles obtained from another class of Orlistat compounds reported previously.^[4b] The two key intermediates, **10a** and **19a**, produced only weakly labeling profiles (including weak FAS labeling), again reinforcing the importance of an *N*-formylated amino ester moiety in the Orlistat structure. However, covalent labeling of other cellular targets could still be readily detected in the fluorescence gel, with different probes generating marginally but noticeably different labeling profiles. This result indicates that our probes targeted both common and unique cellular targets in HepG2 cells, which might have accounted for the subtle differences in their anti-proliferative activities as well. To further identify these potential cellular targets, we performed large-scale affinity pull-down/LCMS analysis of protein lysates obtained from live HepG2 cells treated with each of the probes. Previously, we used a standard, non-cleavable biotin reporter tag to enrich covalently captured proteins and eluted them by boiling them in the presence of an SDS-containing buffer.^[4a] However, under such harsh denaturing conditions, both endogenously biotinylated and highly expressed cellular proteins (nonspecifically bound to the avidin beads) were still present in the eluent even after repeated washes, resulting in an unacceptable number of false positives and greatly interfering with the identification of low-abundance cellular targets. In this study, improvement was made by making use of an azobenzene-functionalized biotinylated linker (compound **6** in Figure 1a; for the synthesis, see the Supporting Information, Scheme S1),^[15] which allows selective release of probe-labeled proteins under mild elution conditions (25 mM $Na_2S_2O_4$) that are compatible with mass spectrometric analysis. Consequently, fewer false positives and more reliable putative protein hits were obtained in our assay. Briefly, as summarized in Figure 1a, cellular lysates containing protein that has been covalently labeled with the Orlistat-like probe, were treated with the cleavable biotin–diazo–azide linker (**6**) under standard click chemistry conditions, precipitated with acetone, washed with methanol, solubilized with an SDS buffer, followed by affinity purification with Neutra-vidin beads and SDS-PAGE gel separation. The entire lane from each pull-down experiment was excised into 10 contiguous gel slices, which were subsequently processed individually for in-gel trypsin digestion as described in the Experimental Section. As negative controls, the entire large-scale proteomic experiment (from cell treatment to LCMS analysis) was repeated with dimethyl sulfoxide. The peptides obtained from each gel slice were eluted and subjected to nano-LC-MS/MS analysis. The LC-MS/MS data were

Table 1. Potentially unique proteins identified by mass spectrometry.^[a]

Gene symbol	Protein name	Probe	Localization	Function
HLA-A	HLA class I histocompatibility antigen, A-68 alpha chain	1a	membrane	host-virus interaction, immune response
PFN1	Profilin-1	1a	cytoplasm	cytoskeletal protein binding
RPL22	60S ribosomal protein L22	1a	cytoplasm, nucleus	protein metabolism
MIF	Macrophage migration inhibitory factor	1a	cytoplasm	cell proliferation, signal transduction
RPL12	60S ribosomal protein L12	1a	nucleus	protein metabolism
PC	Pyruvate carboxylase, mitochondrial	1a	mitochondrion	gluconeogenesis, lipid synthesis
PGM1	Phosphoglucomutase 1	1a	cytoplasm	glucose metabolism
BCAP31	B-cell receptor-associated protein 31	1a	ER, nucleus	transport, apoptosis
CLTCL1	Isoform 1 of Clathrin heavy chain 2	1b	cytoplasm	receptor-mediated endocytosis
PFKM	Isoform 2 of 6-phosphofructokinase, muscle type	1b	n/a	glycolysis
TPP2	Tripeptidyl-peptidase 2	1b	cytoplasm, nucleus	proteolysis
HLA-B	HLA class I histocompatibility antigen, B-59 alpha chain	1c	membrane, cytoplasm, nucleus	immune response
PTGES2	Prostaglandin E synthase 2	1c	membrane	fatty acid biosynthesis, lipid synthesis
ANP32A	Acidic leucine-rich nuclear phosphoprotein 32 family member A	1c	ER, nucleus, cytoplasm	tumor suppressor, transcriptional repression
ATP1B3	Sodium/potassium-transporting ATPase subunit beta-3	1c	membrane	transport
P4HB	cDNA FLJ59430, highly similar to Protein disulfide-isomerase	1c	ER	cell redox homeostasis
HLA-C	HLA class I histocompatibility antigen, Cw02 alpha chain	1d	membrane	immune response
EIF3E	Eukaryotic translation initiation factor 3 subunit E	1d	cytoplasm, nucleus	protein biosynthesis
NOP56	Nucleolar protein 56	1d	nucleus	ribosome biogenesis
MYOF	Isoform 5 of Myoferlin	1d	membrane	phospholipid binding
GNAI2	Guanine nucleotide-binding protein G(i), alpha-2 subunit	1e	membrane	signal transduction
SCARB1	Scavenger receptor class B member 1	1e	membrane	receptor for phospholipids, cholesterol ester, lipoproteins, phosphatidylserine
STAT3	Signal transducer and activator of transcription 3	1f	cytoplasm, nucleus	transcription regulation
SCAMP3	Secretory carrier-associated membrane protein 3	1f	membrane	transport
TMEM48	Isoform 3 of Nucleoporin NDC1	1f	nucleus	transport
MYH9	Isoform 2 of Myosin-9	1f	cytoplasm, nucleus	cytokinesis
SEC61A2	Sec61 alpha form 2 isoform b	1f	ER	transport
LMNA	Isoform C of Lamin-A/C	1g	nucleus	muscle organ development
BZW1	Basic leucine zipper and W2 domain-containing protein 1	1h	cytoplasm, nucleus	transcription regulation
DNAJC11	Isoform 3 of DnaJ homolog subfamily C member 11	1h	n/a	unknown
RAB4B	Ras-related protein Rab-4B	1h	membrane	vesicular trafficking
NIT2	Omega-amidase NIT2	1h	cytoplasm	hydrolase, metabolism
KIAA0368	KIAA0368 protein	1h	ER, centrosome	protein metabolism
GTF2I	Isoform 1 of General transcription factor II-I	1h	cytoplasm, nucleus	transcription regulation
ARF1	ADP-ribosylation factor 1	1h	Golgi	transport, signal transduction
TOP2B	DNA topoisomerase 2-beta	1h	nucleus	transcription regulation
LY6K	Lymphocyte antigen 6 K	1j	membrane, nucleus	useful as a tumor biomarker
LYPLA2	Acyl-protein thioesterase 2	1j	cytoplasm	fatty acid biosynthesis, lipid synthesis
GNAO1	Guanine nucleotide-binding protein G(o) subunit alpha	1j	membrane	signal transduction
ATP2A1	SERCA1B of Sarcoplasmic/endoplasmic reticulum calcium ATPase 1	2a	ER	apoptosis in response to ER stress
SH3KBP1	SH3 domain-containing kinase-binding protein 1	2a	cytoplasm	signal transduction
PLEC1	Isoform 1 of Plectin	2b	cytoplasm	actin binding
ESYT2	Isoform 4 of Extended synaptotagmin-2	3b	membrane	unknown

[a] 44 potentially unique proteins were listed. References are given in the Supporting Information. n/a = not available.

searched against the IPI (International Protein Index) human protein database using an in-house MASCOT server for protein identification. All proteins were identified by a minimum score of 40 and at least two unique peptides. Based on these criteria, around 200 proteins on average

were identified for each of the seventeen Orlistat probes used (Figure 1d, top). Details of the identified protein hits, including their accession numbers, emPAI values, and protein masses, are listed in the Supporting Information (Table S2, Table 1 lists the unique proteins identified). A

total of sixty proteins were identified in all of our probes, which may constitute the common cellular targets for these probes (for a detailed list and relevant references, please see the Supporting Information). These include well-known serine-type proteins, such as enolases (ENO1, ENO3), elongation factors (EEF2, EEF1A1, and EEF1G) and cysteine-type proteins, such as transferrin receptor protein (TFRC), ubiquitin-like modifier-activating enzyme (UBA1), and protein disulfide isomerase (PDIA6), and several lipid-metabolism-related proteins, such as 3-hydroxyacyl-CoA dehydrogenase type-2 (HSD17B1), triosephosphate isomerase, and trans-2,3-enoyl-CoA reductase. Five of our previously identified targets against **1a** (FASN, GAPDH, β -tubulin, Annexin A2, and HSP90AB1),^[4a] also emerged as common hits for our new probes. Not surprisingly, some other lipid- and/or fatty-acid-metabolism-related proteins, such as palmitoyl-protein thioesterase (PPT1), carnitine *O*-palmitoyltransferase (CPT1A), ATP-citrate synthase (ACLY), dihydrolipoyl dehydrogenase (DLD), acyl-CoA dehydrogenases (ACADM, ACADVL), fatty aldehyde dehydrogenase (ALDH3A2), sterol *O*-acyltransferase (SOAT1), long-chain acyl-CoA synthetase (SLC27A2), acetyl-CoA acetyltransferases (ACAT1), lysophospholipid acyltransferase (MBOAT7), were also pulled-down by most (but not all) of our Orlistat probes.^[16–22]

Recent advances in quantitative mass spectrometry have now allowed the direct evaluation of drug–protein interactions based on the relative peak intensity (or the spectra count) of proteins/peptides obtained from a mass spectrometer.^[23] Although semi-quantitative at best, this evaluation provides a very simple and quick method to evaluate the relative binding efficiency of a drug against its protein target.^[24] Specifically, the so-called emPAI (Exponentially Modified Protein Abundance Index) MS quantitation approach provides an estimate of protein concentration from the number of peptide sequences of a protein identified by tandem mass spectrometry.^[24c,d] The abundance of an identified protein in a given pull-down sample relative to the abundance of the same protein in all pull-down samples was then calculated as the ratio of its emPAI value over the sum of the emPAI values for that protein in all seventeen samples. These ratios were then plotted in a heat map for all protein/probe combinations (see the Supporting Information, Figure S2). As shown in Figure 1d, bottom, FAS which was successfully pulled down by all seventeen Orlistat probes showed varied relative percentage abundance values ranging from as low as 3.0% (with probe **3a**) to as high as 12.8% (with probe **1e**), thereby indicating small but relatively significant differences in the relative binding affinity between this protein and the different Orlistat probes. It should be noted that all MS-based results obtained herein (including all the putative protein hits identified and their emPAI values) should only be used as preliminary data. In our current study, improvement on our previous affinity pull-down procedures was made.^[4a] Nevertheless, owing to the highly complex cellular environment, the intrinsic limitation of affinity pull-down assay and mass spectrometry,^[23,24]

false positives/non-specific proteins binders could be minimized but not eliminated entirely from our results. Consequently, proper follow-up studies and validation experiments will be needed before any biological conclusions can be made for some of these protein hits.

One of the questions we were interested in addressing was whether subtle chemical modifications of the Orlistat structure led to changes in its cellular targets, which was already suggested by the earlier *in situ* proteome-profiling experiments (Figure 1c). If so, one would expect that unique proteins targeted by each of the seventeen Orlistat probes could be identified from our affinity pull-down/LCMS experiments. Upon closer examination of our MS results, we found a total of forty-four unique proteins from twelve of the seventeen Orlistat probe used (Figure 1d, bottom, and Table 1). Among those proteins are several HLA (human leukocyte antigen) class I antigens that are part of the genetic region known as the major histocompatibility complex (MHC) class I proteins,^[25] and G proteins (guanine-nucleotide-binding proteins) which belong to the larger group of enzymes called GTPases.^[26] Specifically, HLA-A, HLA-B, and HLA-C were targeted uniquely by **1a**, **1c**, **1d**, and GNAI2, GNAO1 were detected only with **1e**, **1j**, respectively. Interestingly, serine exopeptidase TPP2 (tripeptidyl-peptidase 2), which is essential for some MHC class I antigen presentation,^[27] was selectively pulled-down by **1b**. STAT3 (signal transducer and activator of transcription 3), which has recently been identified as a tumor suppressor,^[28] was uniquely pulled down by **1f**. NIT2, an omega-amidodicarboxylate amidohydrolase and a known tumor-suppressor protein,^[29] was pulled down only by **1h**. Again, we caution that these MS-derived results are only preliminary findings, and need to be further confirmed with suitable validation experiments. Nevertheless, our data concludes that subtle chemical modifications could change the selectivity profiles/cellular targets of Orlistat, and some of its analogues may be further developed into drugs targeting some of the unique proteins mentioned above.

Design and Synthesis of AGT/SNAP-Orlistat Bioconjugates as Organelle-Targetable Probes

Sub-cellular targeting of a drug, whereby the drug is delivered to a specific organelle inside living cells and subsequently retained there (thus greatly increasing the effective concentration of the drug), is expected to not only improve its *in vivo* efficacy but also minimize its off-target effects and cytotoxicity.^[30] A number of drug-delivery vehicles, including the mannose cluster for mannose-receptor interaction targeting the endolysosomal pathway,^[11a] cell-penetrating and cell-localization peptides,^[11b,c] have been successfully used for sub-cellular delivery. We were particularly intrigued by the AGT/SNAP-tag method, which is widely used in the bioimaging field for highly efficient *in vivo* protein labeling using benzylguanine (BG)-containing small-molecule probes.^[12,31] The Johnsson group and other groups recently adopted this method for the sub-cellular delivery of small-

molecule-based fluorescence sensors for the sensitive detection of zinc(II),^[31b] calcium(II),^[31c,d] and H₂O₂^[11d] in cultured cells. We were interested to know whether the same concept could also be applied for sub-cellular drug delivery. Because FAS expresses mostly in the endoplasmic reticulum (ER), modifying Orlistat to be delivered and retained in the ER should in principle greatly improve the drug's anti-tumor activity (both in potency and selectivity). As shown in Scheme 3, in a proof-of-principle study, we envisaged a drug-delivery system consisting of two critical components: a benzylguanane (BG)-derivatized Orlistat (**4**; Scheme 3c) and a model mammalian cell line over-expressing a SNAP protein fused to a desired protein-localization sequence (PLS). Organelle-targetable probe **4** was designed on the basis of our previous findings that, having a terminal alkyne handle on the right-hand aliphatic chain and structural variations on the left-hand aliphatic chain of Orlistat do not significantly interfere with the drug's inhibition of FAS.^[4a,b] Therefore, we were hopeful that once **4** enters the cells and becomes conjugated by the SNAP protein (Scheme 3b), the resulting AGT/SNAP-Orlistat conjugate would be locally "concentrated" and retained in the desired sub-cellular organelle (Scheme 3a). Subsequently, sub-cellular protein targeting may take place. Compound **4** was conveniently prepared using click chemistry between benzylguanane azide (**24**), synthesized in two steps from 6-chloroguanine (see the Supporting Information, Scheme S2), and the previously reported compound **5** (Scheme 3c).^[4b]

Next, we confirmed that BG-containing Orlistat **4** could indeed serve as a substrate of AGT/SNAP and be successfully conjugated (i.e. Scheme 3b, Step I). As shown in Figure 2, recombinantly purified hexahistidine-tagged AGT protein (His-AGT), pre-incubated with **4** in PBS for 4 hours at room temperature, was shown to completely stop the fluorescence labeling between His-AGT and its natural sub-

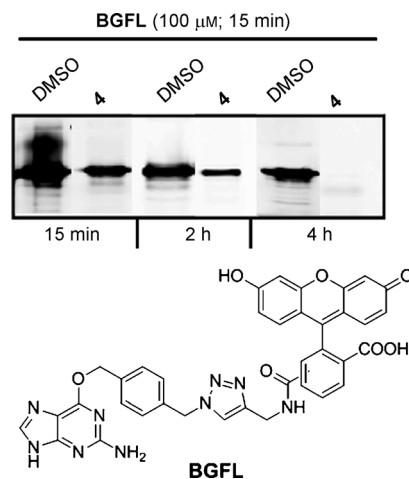
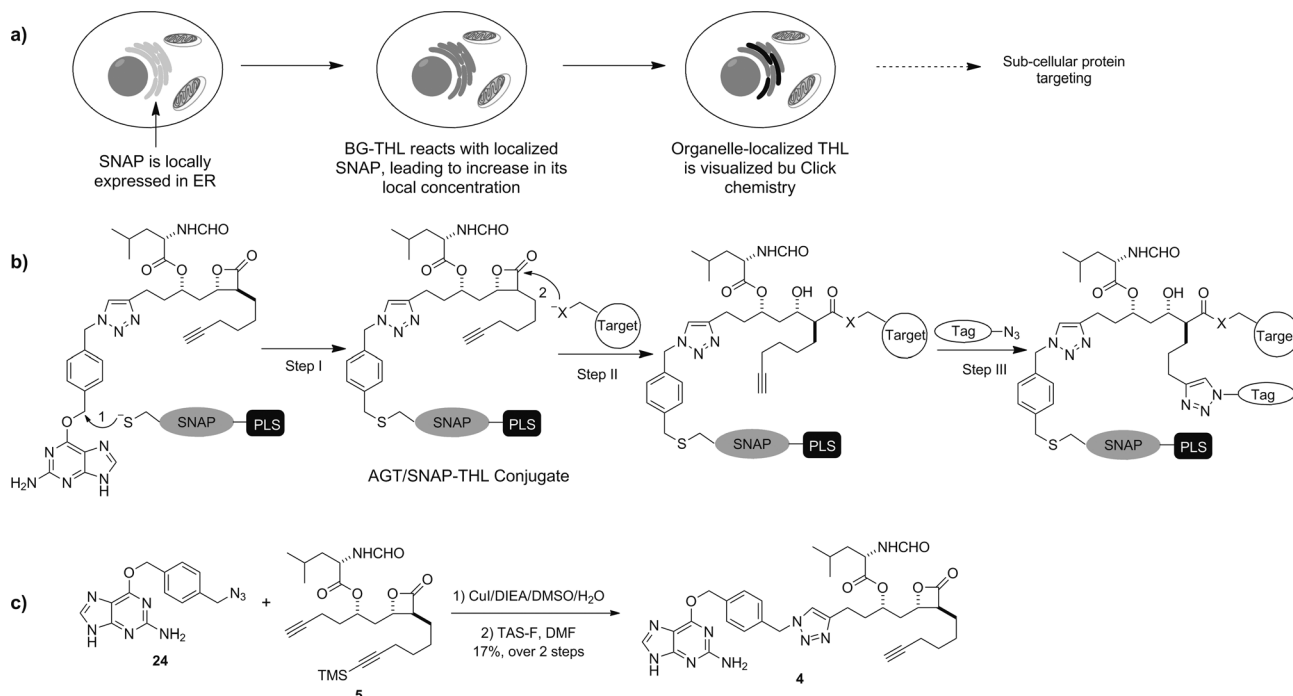


Figure 2. Competition assay for AGT labeling with **4**. Aliquots taken from the reaction mixture at the indicated time and incubated with BGFL (100 μ M) for 15 minutes, followed by SDS-PAGE and in-gel fluorescence scanning.



Scheme 3. a) Principle of AGT/SNAP-tag fusion strategy for sub-cellular protein targeting using a cell-permeable, benzylguanane (BG)-containing Orlistat analogue (**4**). b) Bioconjugation reaction of AGT/SNAP+BG-Orlistat that occurs inside living cells, followed by sub-cellular protein targeting/bio-imaging. c) Schematic showing of click chemistry-facilitated synthesis of the organelle-targeting, BG-containing Orlistat probe (**4**). DMSO = dimethyl sulfoxide.

strate, **BGFL**, thereby indicating the successful formation of the desired AGT/SNAP-Orlistat (Scheme 3b). Further confirmation was obtained from ESI-Q-TOF mass analysis (Table 2); a mass shift of 535 between the untreated His-AGT and (His-AGT+**4**) labeling reaction was observed, which is consistent with the calculated mass of the AGT/SNAP-Orlistat conjugate. The reactive β -lactone ring in Orlistat also remained intact after conjugation.

Table 2. Observed mass peaks for ESI-Q-TOF mass analysis of His-AGT with and without **4**.^[a]

Sample	MW [Da]	Mass difference
His-AGT	23071	
His-AGT+ 4	23606	535

[a] For original mass spectra, see the Supporting Information.

Lastly, we assessed whether the direct application of **4** to live mammalian cells leads to successful localization and retention of the Orlistat probe in the desired sub-cellular organelle. However, we were unable to carry out experiments directly in HepG2 cancer cells, because an AGT-deficient cell-line is currently not available,^[32] and the intrinsically low transfection efficiency of HepG2 cells also precluded the accumulation of a sufficient amount of transiently expressed PLS-SNAP in the cells. Therefore, we used an AGT-deficient CHO-9 cell-line instead. Sub-cellular expression of AGT-SNAP protein was performed by transient transfection of the CHO-9 cells with mammalian DNA constructs containing the AGT-SNAP gene fused to the different protein localization sequences (PLS; including membrane, ER, and nucleus). Forty eight hours later, after the proteins were successfully expressed and detected in the corresponding organ-

elles (Figure 3; green channels), compound **4** was directly applied to the media and the (SNAP+**4**) conjugation reaction was left to proceed for another four hours followed by extensive washing of the cells (to remove excessive probe). Subsequently, in situ click chemistry was carried out in these live cells, using a previously reported procedure,^[4a] to visualize the localization/retention of **4** (Scheme 3b, Step III). As shown in Figure 2 (red channels), the successful accumulation of **4** in the desired organelles (mitochondria, ER, and nucleus), as guided by the localization of AGT-SNAP, was observed (see the merged images of the green and red channels). Cells transfected with a control plasmid containing AGT/SNAP gene without a protein localization sequence displayed uniform fluorescence labeling throughout the entire cell (data not shown). Taken together, these data show that the Orlistat probe **4** could be successfully delivered/retained in sub-cellular organelles by using the AGT/SNAP-tag strategy.^[12d] At present, owing to the lack of a suitable AGT-deficient HepG2 cell line, we were unable to carry out subsequent in situ proteome profiling/LCMS experiments for target identification. However, as a proof-of-concept experiment, we believe the AGT/SNAP-tag strategy represents an interesting and viable tool for sub-cellular drug delivery and organelle targeting. It might even be used in the future for in vivo organelle proteomics applications.^[33]

Conclusions

We have synthesized and evaluated a set of Orlistat-like compounds for their anti-proliferative activity in HepG2 cancer cells. Our results showed some of the analogues (**1a–1d**, **1f**, **2a**, **2d**, **3a**, and **3c**) displayed comparable activities

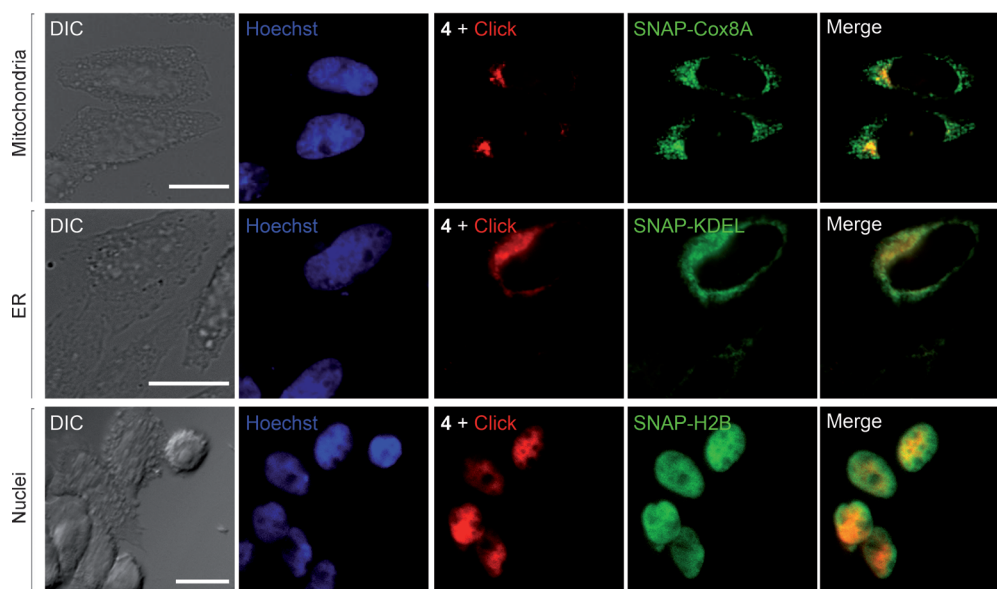


Figure 3. Images of CHO-9 cells expressing AGT-SNAP-tag in mitochondria (top), ER (center), or nuclei (bottom), then treated with **4**, fixed, permeabilized, clicked with rhodamine-azide, and imaged (red channels). Cell nuclei were stained with Hoechst (blue channels), anti-FLAG M2 primary antibody, followed by FITC-conjugated antimouse IgG antibody to detect AGT/SNAP protein (green channels). Red and Green channels were overlaid, giving merged images shown. Scale bar = 10 μ m. PLS: Cox8A (mitochondria); KDEL (ER); H2B (nucleus).

when compared to the parent drug Orlistat, whilst others showed marginally weaker activities. Subsequent *in situ* proteome-activity profiling, followed by large-scale affinity pull-down/LCMS identifications of putative protein hits enabled us to identify potential common and unique targets and to assess their relative binding to our probes, thus providing some preliminary structure-activity-relationship (SAR) information. This chemical-proteomics approach may be used for the discovery of new cellular targets of Orlistat and for the design of better Orlistat analogues. It may also provide a general method for both on- and off-target identification of other suitable drugs. Finally, in order to further improve the cellular activity of Orlistat, we have successfully applied the well-established AGT/SNAP-tag technology to a benzyl-guanine (BG)-containing Orlistat variant (**4**), and in a proof-of-concept bioimaging experiment, showed the drug could be delivered and effectively retained in different sub-cellular organelles of living cells. Owing to the lack of an AGT-deficient HepG2 cell line, subsequent *in situ* proteome profiling and pull-down/LCMS experiments were not possible at this stage.

Experimental Section

Chemicals and Antibodies

Orlistat (98%), Tris(2-carboxyethyl) phosphine (TCEP), the click chemistry ligand, and tris[(1-benzyl-1H-1,2,3-triazol-4-yl)methyl]amine ("ligand") were purchased from Sigma-Aldrich. Hoechst33342 was purchased from Invitrogen. Monoclonal ANTI-FLAG M2 antibody was purchased from Sigma. The bacterial His-AGT plasmid, mammalian plasmids FLAG-Cox8A-SNAP, FLAG-H2B-SNAP, FLAG-KDEL-SNAP, FLAG-NK1R-SNAP, mCherry-Cox8A, and mCherry-KDEL were generous gifts from Christopher J. Chang (University of California, Berkeley). AGT-deficient CHO-9 cell line was a generous gift from the Institute of Toxicology, University of Mainz (Germany). Recombinant expression and purification of His-AGT protein was as previously reported.^[11d]

Cell-Culture Conditions

HepG2 cells were grown in DMEM (Invitrogen, Carlsbad, CA) containing 10% heat-inactivated fetal bovine serum (FBS; Gibco Invitrogen), 100 U mL⁻¹ penicillin, and 100 µg mL⁻¹ streptomycin (Thermo Scientific, Rockford, IL) and maintained in a humidified 37°C incubator with 5% CO₂. CHO-9 cells were maintained in F12-Nutrient Mixture (Invitrogen) supplemented with 5% fetal bovine serum and 100 U/mL penicillin and 100 µg mL⁻¹ streptomycin.

Cell-Proliferation Assay

Cell viability was determined using the XTT colorimetric cell-proliferation kit (Roche) following the manufacturer's guidelines. Briefly, cells were grown to 20–30% confluence (because they will reach approximately 90% confluence within 48 to 72 h in the absence of drugs) in 96-well plates under the conditions described above. The medium was aspirated, washed with PBS, and then treated, in duplicate, with 0.1 mL of the medium containing different concentrations of the probe (1–50 µM) or Orlistat (1–50 µM; as a positive control). Probes were applied from DMSO stocks whereby DMSO never exceeded 1% in the final solution. The same volume of DMSO was used as a negative control. Fresh medium, along with the probes and Orlistat, were added every 24 h. After a total treatment time of 72 h, proliferation was assayed using the XTT colorimetric cell proliferation kit (Roche) following manufacturer's guidelines (read at 450 nm). Data represent the average (±s.d.) of two trials.

In Situ Proteomic Profiling

Cells were grown to 80–90% confluence in 24-well plates under the conditions described above. The medium was removed, and then cells were washed twice with cold PBS, and treated with 0.5 mL of DMEM-containing probe (20 µM). All compounds were solubilized in DMSO. To avoid adverse effects on cell growth, the final DMSO concentration in the assay never exceeded 1% in cultivation medium. Medium containing 1% DMSO was used as a negative control. After incubation, the growth medium was aspirated, and cells were washed twice with PBS to remove the excess probe, trypsinized, and pelleted at 1,000 rpm for 10 min, washed twice with PBS, and re-suspended in PBS (100 µL). Cells were homogenized by sonication, and diluted to ~1 mg/mL with PBS. To initiate the click chemistry reaction, 20 µL of freshly premixed solution containing rhodamine-azide (100 µM final concentration), TCEP (1 mM final concentration), ligand (100 µM final concentration), and CuSO₄ (1 mM final concentration) were added. The reaction was incubated at 10°C for 2 h with gentle mixing. Termination of the reaction was done by addition of pre-chilled acetone (0.5 mL). The resulting solution was then placed at –20°C for 30 min, followed by centrifugation (13,000 rpm × 10 min) at 4°C. The supernatant was discarded and the precipitated protein pellets were washed with pre-chilled methanol (2 × 200 µL), air-dried for 10 min, resuspended in 1 × standard reducing SDS-loading buffer (25 µL) then heated for 10 min at 95°C. Finally, the protein sample (ca. 50 µg/lane) was loaded onto 4% to 15% gradient precast SDS-PAGE (16 × 20 cm), separated, followed by *in-gel* fluorescence scanning with a Typhoon 9410 Variable Mode Imager scanner (GE Amersham).

Pull-Down and Mass Spectrometry Identification

For proteomic experiments, living HepG2 cells (T75 culturing flask) labeled in growth media with probes or DMSO (negative control) were harvested, washed, and homogenized in PBS. CuAAC reagents were added at the same concentrations as described above, except that biotin-diazo-azide **6** was substituted for rhodamine-azide. Acetone-precipitated and methanol-washed protein pellets were solubilized in PBS containing 0.1% (w/v) SDS by brief sonication. Insoluble materials were precipitated by centrifugation (13,000 g × 10 min) at 4°C. The supernatants were then incubated with gentle shaking at 4°C overnight with Neutravidin agarose beads (50 µL mg⁻¹ protein, Prod # 29204, Thermo Scientific, USA) which have been pre-washed twice with PBS. After centrifugation, the bead/complexes were washed extensively 4 times with 1% (w/v) SDS in PBS, three times with PBS, and twice with 250 mM ammonium bicarbonate (ABC). Beads were re-suspended in 500 µL of 8 M urea, and then 25 µL of 200 mM TCEP and 25 µL of 400 mM iodoacetamide were added for capping of the reactive cysteine residues. After 30 min, the beads were washed twice with 250 mM of ABC. Elution of bound proteins from the beads was then performed with a total of 400 µL freshly prepared elution buffer (0.5% SDS, 25 mM Na₂S₂O₄ in 50 mM ABC) by rocking for 1 h at room temperature. Protein samples were concentrated using an YM-10 Centricon spin column (Millipore, USA). Following SDS-PAGE separation, protein bands were visualized by Coomassie blue/silver staining. Gel lanes corresponding to both DMSO-treated and probe-treated samples were then each cut into 10 slices. Subsequent trypsin digestion (using In-Gel Trypsin Digestion Kit, Pierce Co., USA) and peptide extraction (with 50% acetonitrile and 1% formic acid) generated a total of 10 LCMS samples for each pull-down experiment. All samples were dried *in vacuo* and stored at –20°C until LCMS analysis. Each LCMS sample was re-suspended in 0.1% formic acid for mass spectrometry analysis as previously described.^[34a] Briefly, peptides were separated and analyzed on a Shimadzu UFLC system (Shimadzu, Kyoto, Japan) coupled to an LTQ-FT Ultra (Thermo Electron, Germany). Mobile phase A (0.1% formic acid in H₂O) and mobile phase B (0.1% formic acid in acetonitrile) were used to establish the 60 min gradient comprised of 45 min of 5–35% B, 8 min of 35–50% B, and 2 min of 80% B, followed by re-equilibrating at 5% B for 5 min. Peptides were then analyzed on LTQ-FT with an ADVANCE™ CaptiveSpray™ Source (Michrom BioResources, USA) at an electrospray potential of 1.5 kV. A gas-flow of 2 L min⁻¹, ion-transfer tube temperature of 180°C and collision-gas pressure of 0.85 mTorr were used. The LTQ-FT was set to perform data acquisition in the

positive ion mode as previously described except that the m/z range of 350–1600 was used in the full MS scan.^[34a] The raw data were converted into the mgf format as described previously.^[34b] The database (76708 sequences, 33362815 residues) used for the Mascot search was a concatenated IPI protein database. The database search was performed using an in-house Mascot server (version 2.2.07, Matrix Science, UK) with an MS tolerance of 10 ppm and MS/MS tolerance of 0.8 Da. Two missed cleavage sites of trypsin were allowed. Carbamidomethylation (C) was set as a fixed modification, and oxidation (M) and phosphorylation (S, T, and Y) were set as variable modifications.

In Vitro His-AGT Labeling with (**4**) and Analysis by ESI-Q-TOF MS

His-AGT (2 μ M) was incubated in PBS with 1 μ M of **4** for different lengths of time (15 min, 2 h, and 4 h) at room temperature, then incubated with **BGFL** (100 μ M) for 15 min followed by SDS-PAGE separation, and in-gel fluorescence scanning. The deconvoluted MS data were collected by ESI-Q-TOF mass analysis.

Fluorescence Microscopy

AGT-deficient CHO-9 cells were seeded on sterile 12-mm glass coverslips contained in 24-well plates and left to adhere for 24 h prior to transfection. Transient transfection was carried out according to protocol instructions by using EndoFectin (GeneCopoeia). The medium was replaced 12 h post-transfection. After 36 h, the cells were incubated with **4** (30 μ M) for 4 h in growth medium at culture temperature and 5% CO₂. Medium containing 1% DMSO was used as a negative control. The cells were then washed twice with PBS, and fixed with 4% paraformaldehyde in PBS for 15 min at room temperature, washed with PBS (2 \times 5 min with gentle agitation), and permeabilized with 0.1% Triton-X 100 in PBS for 15 min at room temperature, and washed with PBS (2 \times 5 min with gentle agitation). The cells were blocked with 2% bovine serum albumin (BSA) in PBS for 30 min at room temperature, and washed with PBS (2 \times 5 min with gentle agitation). The cells were then treated with a freshly premixed click chemistry reaction solution of rhodamine-azide (10 μ M final concentration from a 10 mM stock solution in DMSO), TCEP (1 mM final concentration from a 50 mM freshly prepared stock solution in deionized water), TBTA (100 μ M final concentration from a 10 mM stock solution in DMSO), and CuSO₄ (1 mM final concentration from a 100 mM freshly prepared stock solution in deionized water), in PBS for 1 h at room temperature. The cells were washed with PBS (1 \times 5 min with gentle agitation), and cold methanol (1 \times 5 min with gentle agitation), followed by 1% Tween-20 and 0.5 mM of EDTA in PBS (3 \times 2 min with gentle agitation), and with PBS (2 \times 5 min with gentle agitation). The cells were then incubated in PBS containing 0.25 μ g mL⁻¹ of Hoechst for 15 min at room temperature to stain the nuclear DNA, and washed with PBS (2 \times 5 min with gentle agitation) and a final wash with deionized water (1 \times 5 min with gentle agitation) before mounting. For co-localization of SNAP protein expressed, indirect immunofluorescent cytochemical staining was carried out according to the manufacturer's instructions. Cells were blocked with 10% BSA in PBS for 30 min, and washed with PBS (2 \times 5 min with gentle agitation). The cells were incubated with monoclonal Anti-FLAG M2 antibody diluted in 1:2000 in 3% BSA in PBS for 2 h at 37°C, and washed with PBS (3 \times 5 min with gentle agitation). Then secondary antibody goat-anti-mouse IgG-FITC (Santa Cruz) diluted in 1:100 in 3% BSA in PBS for 45 min at 37°C, and washed PBS (2 \times 5 min with gentle agitation). Images were acquired using Observer Z1 (Zeiss, Germany) equipped with a 63X NA1.4 objective and a CoolSNAP HQ2 CCD camera (Photometrics, USA), or LSM 510 META (Zeiss, Germany) equipped with an EC Plan-Neofluar 100 \times NA1.3 objective.

Chemical Synthesis

All chemicals were purchased as reagent grade and used without further purification, unless otherwise noted. Tetrahydrofuran (THF) was distilled over sodium benzophenone and used immediately. All non-aqueous reactions were carried out under nitrogen atmosphere in oven-dried glassware. Reaction progress was monitored by TLC on pre-coated silica plates (Merck 60 F254, 250 μ m thickness) and spots were visualized by ceric ammonium molybdate, basic KMnO₄, or UV light. ¹H NMR and

¹³C NMR spectra were recorded on a Bruker model DPX-500 MHz NMR spectrometer. Chemical shifts are reported in parts per million relative to internal standard tetramethylsilane (Si(CH₃)₄ = 0.00 ppm) or residual solvent peaks (CHCl₃ = 7.26 ppm). Mass spectra were obtained at the center for Chemical Characterization and Analysis at NUS. β -lactone **1a-g**, **2a**, **3a**, **5**, **7b**, **10a**, **19a**, and **22** were synthesized as previously described.^[4]

(S)-(R)-1-[(2R,3R)-3-(hex-5-yn-1-yl)-4-oxooxetan-2-yl]tridecan-2-yl 2-formamidopropanoate (**1h**)

β -lactone **10b** (14 mg, 0.04 mmol), triphenylphosphine (21 mg, 0.08 mmol), *N*-formyl-L-alanine (10 mg, 0.08 mmol) were placed in a round-bottom flask and azeotroped under vacuum with 0.5 mL of xylene for 30 min. Addition of 1 mL dry THF was followed by cooling to 0°C; DIAD (12 μ L, 0.08 mmol) was then added via syringe. The mixture was stirred at 0°C for 10 min, and allowed to warm to ambient temperature. The reaction was monitored by TLC. After the reaction was complete, the mixture was then concentrated in vacuo and purified by flash chromatography on silica gel (20% EtOAc/hexanes) to afford **1h** (7 mg, 36%) as a colorless oil. ¹H NMR (500 MHz, CDCl₃): δ = 8.18 (s, 1H), 6.17 (br s, 1H), 5.04–5.09 (m, 1H), 4.62 (quin, J = 7.6 Hz, 1H), 4.34–4.37 (m, 1H), 3.24 (dt, J = 7.6, 3.8 Hz, 1H), 2.21 (dt, J = 6.3, 2.5 Hz, 2H), 2.19–2.14 (m, 1H), 2.03 (dt, J = 13.9, 5.0 Hz, 1H) 1.96 (t, J = 2.5 Hz, 1H), 1.84–1.54 (m, 10H), 1.45 (d, J = 6.9 Hz, 3H), 1.27 (br s, 17H), 0.88 ppm (t, J = 7.6 Hz, 3H); ¹³C NMR (125 MHz, CDCl₃): δ = 172.2, 170.5, 160.4, 83.9, 74.6, 72.7, 68.7, 56.8, 47.1, 38.7, 33.9, 31.9, 29.6, 29.5, 29.4, 29.3, 29.2, 27.9, 27.1, 25.7, 25.2, 22.7, 18.2, 18.1, 14.1 ppm; ESI-MS: (m/z) calcd for C₂₆H₄₃NO₅ [M+Na]⁺ 472.3, found 472.2.

(R)-1-[(2R,3R)-3-(hex-5-yn-1-yl)-4-oxooxetan-2-yl]tridecan-2-yl 2-formamidoacetate (**1i**)

Prepared according to the representative Mitsunobu reaction procedure using β -lactone **10b** (14 mg, 0.04 mmol), triphenylphosphine (21 mg, 0.08 mmol), *N*-formyl-glycine (10 mg, 0.1 mmol) and DIAD (12 μ L, 0.08 mmol) in 1.0 mL of THF. Purification by flash chromatography on silica gel (15% EtOAc/hexanes) gave **1i** (8 mg, 46%) as a colorless oil. ¹H NMR (500 MHz, CDCl₃): δ = 8.26 (s, 1H), 6.11 (br s, 1H), 5.10–5.15 (m, 1H), 4.33–4.36 (m, 1H), 4.12 (dd, J = 19.0, 5.7 Hz, 1H), 4.04 (dd, J = 19.0, 5.0 Hz, 1H), 3.23 (dt, J = 7.6, 3.8 Hz, 1H), 2.22 (dt, J = 7.0, 2.5 Hz, 2H), 2.1 (dt, J = 15.1, 7.6 Hz, 1H), 2.03 (dt, J = 14.5, 4.4 Hz, 1H), 1.96 (t, J = 2.5 Hz, 1H), 1.86–1.73 (m, 9H), 1.26 (br s, 14H), 0.88 ppm (t, J = 7.6 Hz, 3H); ¹³C NMR (125 MHz, CDCl₃): δ = 170.5, 169.2, 160.9, 83.8, 74.9, 73.0, 68.8, 56.9, 40.1, 38.9, 34.1, 31.9, 29.6, 29.5, 29.4, 29.32, 29.26, 27.9, 25.7, 25.2, 22.7, 18.1, 14.1 ppm; ESI-MS: (m/z) calcd for C₂₅H₄₁NO₅ [M+H]⁺ 436.3, found 436.2.

(2S)-(R)-1-[(2R,3R)-3-(hex-5-yn-1-yl)-4-oxooxetan-2-yl]tridecan-2-yl 2-formamido-3-methylpentanoate (**1j**)

Prepared according to the representative Mitsunobu reaction procedure using β -lactone **10b** (14 mg, 0.04 mmol), triphenylphosphine (21 mg, 0.08 mmol), *N*-formyl-L-isoleucine (14 mg, 0.08 mmol) and DIAD (12 μ L, 0.08 mmol) in 1.0 mL THF. Purification by flash chromatography on silica gel (15% EtOAc/hexanes) gave **1j** (8 mg, 41%) as a colorless oil. ¹H NMR (500 MHz, CDCl₃): δ = 8.23 (s, 1H), 6.16 (br s, 1H), 5.02–5.03 (m, 1H), 4.61 (dd, J = 8.2, 4.4 Hz, 1H), 4.34–4.37 (m, 1H), 3.23 (dt, J = 7.6, 3.8 Hz, 1H), 2.20–2.15 (m, 3H), 1.93 (t, J = 2.5 Hz, 1H), 1.60–1.25 (m, 30H), 0.96 (d, J = 7.0 Hz, 2H), 0.93 (d, J = 7.6 Hz, 3H), 0.87 ppm (t, J = 6.9 Hz, 3H); IT-TOF-MS: (m/z) calcd for C₂₉H₄₉NO₅ [M+H]⁺ calcd: 491.361, found: 492.288.

(S)-(S)-1-[(2S,3S)-3-hexyl-4-oxooxetan-2-yl]tridecan-2-yl 2-formamidopropanoate (**2b**)

Prepared according to the general Mitsunobu reaction procedure using β -lactone **19a** (13 mg, 0.04 mmol), PPh₃ (47 mg, 0.18 mmol), *N*-formyl-L-alanine (21 mg, 0.18 mmol) and DEAD (27 μ L, 0.17 mmol) in THF (1 mL). Purification by flash chromatography on silica gel (hexanes/EtOAc, 100:0 to 4:1) to give **2b** (13 mg, 73%) as a white solid. ¹H NMR (500 MHz, CDCl₃): δ = 8.18 (s, 1H), 6.21 (br d, J = 6.3 Hz, 1H), 5.05–

5.07 (m, 1H), 4.61–4.67 (m, 1H), 4.30 (m, 1H), 3.21 (dt, $J=7.6$, 3.8 Hz, 1H), 2.15 (dt, $J=7.0$, 2.5 Hz, 3H), 2.00 (dt, $J=15.1$, 4.5 Hz, 1H), 1.93 (t, $J=2.5$ Hz, 1H), 1.80–1.50 (m, 8H), 1.45 (d, $J=6.9$ Hz, 3H), 1.39–1.27 (m, 18H), 0.88 ppm (t, $J=7.0$ Hz, 3H); ^{13}C NMR (125 MHz, CDCl_3): $\delta=172.1$, 170.7, 160.4, 84.7, 74.9, 73.0, 68.1, 57.1, 47.1, 38.9, 34.2, 31.4, 29.3, 29.2, 29.16, 29.0, 28.9, 28.7, 28.4, 27.6, 26.7, 25.1, 22.5, 18.3, 14.4, 14.0 ppm; TOF-MS: (m/z) calcd for $\text{C}_{26}\text{H}_{43}\text{NO}_5$ [$M+\text{Na}$] $^+$ 472.304, found 472.267.

(*S*)-1-[(2*S*,3*S*)-3-hexyl-4-oxooxetan-2-yl]tridec-12-yn-2-yl 2-formamidoacetate (**2c**)

Prepared according to the general Mitsunobu reaction procedure using β -lactone **19a** (12 mg, 0.03 mmol), PPh_3 (45 mg, 0.17 mmol), *N*-formylglycine (18 mg, 0.17 mmol) and DEAD (25 μL , 0.16 mmol) in THF (1 mL). Purification by flash chromatography on silica gel (hexanes/EtOAc, 100:0 to 4:1) to give **2c** (15 mg, 70%) as a colorless oil: ^1H NMR (500 MHz, CDCl_3): $\delta=8.04$ (s, 1H), 6.21 (br s, 1H), 5.09–5.14 (m, 1H), 4.31–4.34 (m, 1H), 4.11 (dd, $J=18.3$, 5.7 Hz, 1H), 4.02 (dd, $J=18.3$, 5.1 Hz, 1H), 3.18–3.22 (m, 1H), 2.17 (dt, $J=6.9$, 2.5 Hz, 2H), 2.10–2.15 (m, 1H), 2.01 (dt, $J=15.2$, 4.2 Hz, 1H), 1.93 (t, $J=2.5$ Hz, 1H), 1.81–1.71 (m, 5H), 1.51 (quin, $J=7.0$ Hz, 2H), 1.41–1.27 (m, 16H), 0.88 ppm (t, $J=6.3$ Hz, 3H); ^{13}C NMR (125 MHz, CDCl_3): $\delta=170.8$, 169.2, 161.0, 84.7, 75.0, 73.0, 68.1, 57.0, 40.1, 38.9, 34.1, 31.4, 29.3, 29.2, 29.0, 28.9, 28.7, 28.4, 27.6, 26.7, 25.1, 22.5, 18.4, 14.0 ppm; TOF-MS: (m/z) calcd for $\text{C}_{25}\text{H}_{41}\text{NO}_5$ [$M+\text{Na}$] $^+$ 458.288, found 458.301.

(2*S*)-(S)-1-[(2*S*,3*S*)-3-hexyl-4-oxooxetan-2-yl]tridec-12-yn-2-yl 2-formamido-3-methylpentanoate (**2d**)

Prepared according to the general Mitsunobu reaction procedure using β -lactone **19a** (12 mg, 0.03 mmol), PPh_3 (45 mg, 0.17 mmol), *N*-formyl-L-isoleucine (27 mg, 0.17 mmol) and DEAD (25 μL , 0.16 mmol) in THF (1 mL). Purification by flash chromatography on silica gel (hexanes/EtOAc, 100:0 to 4:1) to give **2d** (11 mg, 63%) as a white solid. ^1H NMR (500 MHz, CDCl_3): $\delta=8.25$ (s, 1H), 6.05 (br d, $J=8.8$ Hz, 1H), 5.00–5.05 (m, 1H), 4.66 (dd, $J=8.8$, 5.1 Hz, 1H), 4.28 (dt, $J=7.6$, 4.4 Hz, 1H), 3.23 (dt, $J=8.2$, 4.4 Hz, 1H), 2.15 (dt, $J=14.5$, 5.1 Hz, 3H), 2.01 (dt, $J=14.5$, 5.1 Hz, 1H), 1.93 (t, $J=2.5$ Hz, 1H), 1.85–1.25 (m, 26H), 0.96 (d, $J=7.0$ Hz, 3H), 0.95 (d, $J=7.0$ Hz, 3H), 0.88 ppm (t, $J=7.6$ Hz, 3H); ^{13}C NMR (125 MHz, CDCl_3): $\delta=170.9$, 170.7, 160.7, 84.8, 74.6, 72.9, 68.1, 57.1, 55.4, 38.6, 37.6, 33.9, 31.5, 29.3, 29.2, 29.0, 28.9, 28.7, 28.4, 27.7, 26.7, 25.1, 24.9, 22.5, 18.4, 15.6, 14.0, 11.5 ppm; TOF-MS: (m/z) calcd for $\text{C}_{29}\text{H}_{49}\text{NO}_5$ [$M+\text{H}$] $^+$ 492.361, found 492.379.

(*R*)-(S)-1-[(2*S*,3*S*)-3-hexyl-4-oxooxetan-2-yl]tridec-12-yn-2-yl 2-formamido-4-methylpentanoate (**2e**)

Prepared according to the general Mitsunobu reaction procedure using β -lactone **19a** (15 mg, 0.04 mmol), PPh_3 (56 mg, 0.22 mmol), *N*-formyl-D-leucine (34 mg, 0.22 mmol) and DEAD (41 μL , 0.21 mmol) in THF (1 mL). Purification by flash chromatography on silica gel (hexanes/EtOAc, 100:0 to 9:1) followed by a second purification by flash chromatography on silica gel (hexanes/EtOAc, 9:1 to 4:1) to give **2e** (8 mg, 36%) as a white solid. ^1H NMR (500 MHz, CDCl_3): $\delta=8.20$ (s, 1H), 5.91 (br d, $J=5.3$ Hz, 1H), 5.00–5.05 (m, 1H), 4.64–4.69 (m, 1H), 4.34–4.37 (m, 1H), 3.22 (dt, $J=6.9$, 4.4 Hz, 1H), 2.18 (dt, $J=6.9$, 2.5 Hz, 1H), 2.02 (dt, $J=14.5$, 4.5 Hz, 1H), 1.93 (t, $J=2.5$ Hz, 1H), 1.86–1.27 (m, 29H), 0.97 (d, $J=5.0$ Hz, 6H), 0.88 ppm (t, $J=7.0$ Hz, 3H); ^{13}C NMR (125 MHz, CDCl_3): $\delta=172.2$, 170.9, 160.6, 84.7, 74.6, 72.6, 68.1, 57.0, 49.6, 41.5, 38.5, 33.8, 31.5, 29.34, 29.32, 29.2, 29.0, 28.9, 28.7, 27.6, 26.7, 25.6, 25.2, 24.9, 22.8, 22.5, 21.9, 18.4, 14.0 ppm; TOF-MS: (m/z) calcd for $\text{C}_{29}\text{H}_{49}\text{NO}_5$ [$M+\text{H}$] $^+$ 492.361, found 492.344.

(*S*)-(R)-1-[(2*R*,3*R*)-3-hexyl-4-oxooxetan-2-yl]tridec-12-yn-2-yl 2-formamido-4-methylpentanoate (**2f**)

Prepared according to the general Mitsunobu reaction procedure using β -lactone **19b** (15 mg, 0.04 mmol), PPh_3 (43 mg, 0.16 mmol), *N*-formyl-L-leucine (27 mg, 0.17 mmol) and DEAD (25 μL , 0.16 mmol) in THF (1 mL). Purification by flash chromatography on silica gel (hexanes/EtOAc, 100:0 to 4:1) to give **2f** (13 mg, 81%) as a colorless oil: ^1H NMR

(500 MHz, CDCl_3): $\delta=8.20$ (s, 1H), 5.95 (br s, 1H), 5.02–5.04 (m, 1H), 4.66–4.69 (m, 1H), 4.26–4.31 (m, 1H), 3.20–3.24 (m, 1H), 2.17 (dt, $J=6.9$, 2.5 Hz, 2H), 2.02–1.98 (m, 1H), 1.93 (t, $J=2.5$ Hz, 1H) 1.82–1.65 (m, 6H), 1.58–1.48 (m, 4H), 1.28 (br s, 18H), 0.96 (d, $J=6.3$ Hz, 6H), 0.88 ppm (t, $J=6.3$ Hz, 3H); ^{13}C NMR (125 MHz, CDCl_3): $\delta=172.2$, 170.9, 160.6, 84.7, 74.5, 72.5, 68.0, 57.0, 47.6, 41.5, 38.7, 33.8, 31.4, 29.3, 29.2, 29.0, 28.9, 28.7, 28.4, 27.6, 26.7, 25.2, 24.9, 22.8, 22.5, 21.8, 18.3, 14.0 ppm; ESI-MS: (m/z) calcd for $\text{C}_{29}\text{H}_{49}\text{NO}_5$ [$M+\text{Na}$] $^+$ 514.4, found 514.3 [$M+\text{Na}$] $^+$.

(*S*)-(S)-1-[(2*S*,3*S*)-3-hexyl-4-oxooxetan-2-yl]tridecan-2-yl 4-methyl-2-(oct-7-ynamido)pentanoate (**3b**)

Prepared according to the general Mitsunobu reaction procedure using β -lactone **21** (100 mg, 0.28 mmol), PPh_3 (110 mg, 0.42 mmol), acid **22** (106 mg, 0.42 mmol) and DIAD (77 μL , 0.39 mmol) in THF (5 mL). Purification by flash chromatography on silica gel (hexanes/EtOAc, 100:0 to 80:20) to give **3b** (49 mg, 30%) as a white solid. ^1H NMR (500 MHz, CDCl_3): $\delta=5.77$ (d, $J=8.2$ Hz, 1H), 5.00 (m, 1H), 4.59 (dt, $J=8.8$, 5.1 Hz, 1H), 4.27–4.30 (m, 1H), 3.21 (dt, $J=7.6$, 3.8 Hz, 1H), 2.23 (t, $J=7.6$ Hz, 2H), 2.19 (dt, $J=8.0$, 2.5 Hz, 2H), 2.14 (t, $J=7.6$ Hz, 2H), 1.98 (dt, $J=15.2$, 4.4 Hz, 1H), 1.93 (t, $J=2.5$ Hz, 1H), 1.71–1.82 (m, 2H), 1.42–1.67 (m, 14H), 1.26 (br s, 22H), 0.96 (d, $J=5.1$ Hz, 3H), 0.95 (d, $J=5.1$ Hz, 3H), 0.88 ppm (t, $J=7.0$ Hz, 6H); ^{13}C NMR (125 MHz, CDCl_3): $\delta=172.6$, 172.5, 170.7, 84.4, 74.8, 72.4, 68.3, 57.1, 51.0, 41.7, 38.7, 36.3, 34.1, 31.9, 31.5, 29.61, 29.60, 29.5, 29.4, 29.3, 29.0, 28.3, 28.1, 27.7, 26.7, 25.1, 25.01, 25.0, 22.9, 22.7, 22.5, 21.9, 18.2, 14.1, 14.0 ppm; ESI-MS: calcd for $\text{C}_{36}\text{H}_{63}\text{NO}_5$ [$M+\text{H}$] $^+$ 590.5; found 590.4.

(*S*)-(S)-1-[(2*S*,3*S*)-3-(hex-5-yn-1-yl)-4-oxooxetan-2-yl]tridecan-2-yl 4-methyl-2-propionamidopentanoate (**3c**)

Prepared according to the general Mitsunobu reaction procedure using β -lactone **10a** (30 mg, 0.086 mmol), PPh_3 (34 mg, 0.13 mmol), acid **20** (24 mg, 0.13 mmol) and DIAD (26 μL , 0.13 mmol) in THF (1 mL). Purification by flash chromatography on silica gel (10% EtOAc/hexanes) to give **3c** (19 mg, 66%) as a white solid. ^1H NMR (500 MHz, CDCl_3): $\delta=6.25$ (d, $J=8.2$ Hz, 1H), 5.00–5.05 (m, 1H), 4.58–4.62 (m, 1H), 4.28–4.31 (m, 1H), 3.23 (dt, $J=3.8$, 7.6 Hz, 1H), 2.85 (s, 1H), 2.22 (dt, $J=2.5$, 6.3 Hz, 2H), 2.15 (t, $J=8.2$ Hz, 1H), 2.01 (dt, $J=4.4$, 15.2 Hz, 1H), 1.95 (t, $J=2.5$ Hz, 1H), 1.73–1.85 (m, 2H), 1.63–1.68 (m, 3H), 1.54–1.68 (m, 8H), 1.25 (br s, 16H), 0.97 (d, $J=6.3$ Hz, 3H), 0.96 (d, $J=6.3$ Hz, 3H), 0.88 ppm (t, $J=7.0$ Hz, 3H); ^{13}C NMR (125 MHz, CDCl_3): $\delta=171.4$, 170.4, 151.7, 83.9, 76.7, 74.6, 74.1, 72.8, 68.7, 56.9, 51.4, 41.2, 38.7, 34.0, 31.9, 29.6, 29.5, 29.4, 29.3(2), 28.0, 27.1, 25.7, 25.1, 24.9, 22.8, 22.7, 21.8, 18.1, 14.1 ppm. ESI-MS: calcd for $\text{C}_{33}\text{H}_{49}\text{NO}_5$ [$M+\text{H}$] $^+$ 516.4; found 516.1.

(*S*)-(S)-4-(1-(4-((2-*amino*-9*H*-purin-6-yl)methoxy)benzyl)-1*H*-1,2,3-triazol-4-yl)-1-((2*S*,3*S*)-3-(hex-5-yn-1-yl)-4-oxooxetan-2-yl)butan-2-yl 2-formamido-4-methylpentanoate (**4**)

To a mixture of di-alkyne β -lactone **5** (10.2 mg, 0.022 mmol) and BG-azide **24** (6.5 mg, 0.022 mmol) in a mixture of DMSO/ H_2O (3:1, 400 μL) was added CuI (4.2 mg, 0.022 mmol) and DIPEA (8 μL , 0.044 mmol). The reaction mixture was stirred at room temperature for 72 h. The reaction mixture was then diluted with water (1 mL) and extracted with EtOAc (3 \times 1 mL). The combined organic phase was extracted with 1 M EDTA solution (3 \times 1 mL), brine (2 mL) and dried over anhydrous Na_2SO_4 . The product was used in the next step without purification. LC-ESI-MS (m/z) calcd for $\text{C}_{38}\text{H}_{52}\text{N}_9\text{O}_6\text{Si}$ [$M+\text{H}$] $^+$ 758.4, found 758.4. To a solution of the above mixture in DMF (200 μL) was added a solution of tris(dimethylamino)sulfonium difluorotrimethylsilicate (TAS-F) (8.0 mg, 0.029 mmol) in DMF (200 μL). The reaction mixture was stirred at room temperature for 12 h. The reaction mixture was diluted with water (500 μL) and the aqueous phase was extracted with EtOAc (3 \times 1 mL). The combined organic phase was washed with brine (1 mL) and dried over anhydrous Na_2SO_4 . The residue was purified by preparative HPLC (Phenomenex Luna C18, 5 μm , 50 \times 3 mm; 0–10 min, 20–95% CH_3CN ; 10–12 min, 100% CH_3CN ; flow rate: 0.5 mL min^{-1}) to give **4** (2.6 mg, 17% yield over two steps) as a colorless oil. ^1H NMR (500 MHz, CDCl_3):

δ = 7.99 (s, 1H), 7.63 (s, 1H), 7.50 (d, J = 7.6 Hz, 2H), 7.41 (s, 1H), 7.24 (d, J = 7.6 Hz, 2H), 5.62 (d, J = 14.5 Hz, 1H), 5.52–5.55 (m, 1H), 5.43 (d, J = 12 Hz, 1H), 5.38 (d, J = 14.5 Hz, 1H), 4.94 (br s, 1H), 4.85 (br s, 1H), 4.49 (br s, 1H), 4.27 (dt, J = 8.2, 4.4 Hz, 1H), 3.20 (dt, J = 8.3, 3.8 Hz, 1H), 2.79 (t, J = 6.3 Hz, 1H), 2.17–2.20 (m, 2H), 2.09–2.15 (m, 2H), 2.00–2.07 (m, 2H), 1.95 (t, J = 2.5 Hz, 1H), 1.51–1.77 (m, 5H), 0.97 (d, J = 6.3 Hz, 3H), 0.94 ppm (d, J = 6.3 Hz, 3H). LC-TOF-MS (m/z) calcd for $C_{35}H_{43}N_9O_6$ [$M+H$]⁺ 686.3336, found 686.3423.

Acknowledgements

This work was supported by the National Research Foundation (NRF), Competitive Research Program (R143-000-218-281; NRF-G-CRP 2007-04). We gratefully acknowledge a generous gift of plasmids from Prof. Christopher J. Chang (University of California, Berkeley). We thank Jigang Wang for technical assistance and Dr. Siu Kwan Sze (Nanyang Technological University, Singapore) for advice and support for LCMS experiments.

- [1] a) L. Sleno, A. Emili, *Curr. Opin. Chem. Biol.* **2008**, *12*, 46–54; b) B. Lomenick, R. W. Olsen, J. Huang, *ACS Chem. Biol.* **2011**, *6*, 34–46.
- [2] a) B. F. Cravatt, G. M. Simon, J. R. 3rd. Yates, *Nature* **2007**, *450*, 991–1000; b) U. Rix, G. Superti-Furga, *Nat. Chem. Biol.* **2009**, *5*, 616–624; c) M. Bantscheff, A. Scholten, A. J. Heck, *Drug Discovery Today Drug Disc. Today* **2009**, *14*, 1021–1029; d) K. Wierzbza, M. Muroi, H. Osada, *Curr. Opin. Chem. Biol.* **2011**, *15*, 57–65.
- [3] a) M. J. Evans, B. F. Cravatt, *Chem. Rev.* **2006**, *106*, 3279–3301; b) M. Fonović, M. Bogyo, *Curr. Pharm. Des.* **2007**, *13*, 253–261; c) M. Uttamchandani, J. Li, H. Sun, S. Q. Yao, *ChemBioChem* **2008**, *9*, 667–675; d) T. Böttcher, M. Pitscheider, S. A. Sieber, *Angew. Chem.* **2010**, *122*, 2740–2759; *Angew. Chem. Int. Ed.* **2010**, *49*, 2680–2698; e) E. E. Carlson, *ACS Chem. Biol.* **2010**, *5*, 639–653.
- [4] a) P.-Y. Yang, K. Liu, M. H. Ngai, M. J. Lear, M. R. Wenk, S. Q. Yao, *J. Am. Chem. Soc.* **2010**, *132*, 656–666; b) M. H. Ngai, P.-Y. Yang, K. Liu, Y. Shen, S. Q. Yao, M. J. Lear, *Chem. Commun.* **2010**, 46, 8335–8837; c) P.-Y. Yang, M. Wang, K. Liu, M. H. Ngai, O. Sheriff, M. J. Lear, S. K. Sze, C. Y. He, S. Q. Yao, submitted.
- [5] Y. Liu, M. P. Patricelli, B. F. Cravatt, *Proc. Natl. Acad. Sci. USA* **1999**, *96*, 14694–14699.
- [6] For other β -lactone related ABPs, see: a) T. Böttcher, S. A. Sieber, *Angew. Chem.* **2008**, *120*, 4677–4680; *Angew. Chem. Int. Ed.* **2008**, *47*, 4600–4603; b) T. Böttcher, S. A. Sieber, *J. Am. Chem. Soc.* **2008**, *130*, 14400–14401; c) T. Böttcher, S. A. Sieber, *ChemBioChem* **2009**, *10*, 663–666; d) T. Böttcher, S. A. Sieber, *ChemMedChem* **2009**, *4*, 1260–1263; e) Z. Wang, C. Gu, T. Colby, T. Shindo, R. Balamurugan, H. Waldmann, M. Kaiser, R. A. van der Hoorn, *Nat. Chem. Biol.* **2008**, *4*, 557–563; f) F. J. Dekker, O. Rocks, N. Vartak, S. Menninger, C. Hedberg, R. Balamurugan, S. Wetzel, S. Renner, M. Gerauer, B. Schölermann, M. Rusch, J. W. Kramer, D. Rauh, G. W. Coates, L. Brunsveld, P. I. Bastiaens, H. Waldmann, *Nat. Chem. Biol.* **2010**, *6*, 449–456.
- [7] US Food and Drug Administration. Orlistat (marketed as Alli and Xenical) Information (online). Available from URL: <http://www.fda.gov/Drugs/DrugSafety/PostmarketDrugSafetyInformationforPatientsandProviders/ucm180076.htm> (Accessed 2010 Nov. 15).
- [8] a) S. J. Kridel, F. Axelrod, N. Rozenkrantz, J. W. Smith, *Cancer Res.* **2004**, *64*, 2070–2075; b) C. D. Browne, E. J. Hindmarsh, J. W. Smith, *FASEB J.* **2006**, *20*, 2027–2035; c) J. L. Little, F. B. Wheeler, D. R. Fels, C. Koumenis, S. J. Kridel, *Cancer Res.* **2007**, *67*, 1262–1269; d) L. M. Knowles, C. Yang, A. Osterman, J. W. Smith, *J. Biol. Chem.* **2008**, *283*, 31378–31384; e) M. A. Carvalho, K. G. Zecchin, F. Seguin, D. C. Bastos, M. Agostini, A. L. C. A. Rangel, S. S. Veiga, H. F. Raposo, H. C. F. Oliveira, M. Loda, R. D. Coletta, E. Graner, *Int. J. Cancer* **2008**, *123*, 2557–2565; f) C. P. Pallasch, J. Schwamb, S. Königs, A. Schulz, S. Debey, D. Kofler, J. L. Schultze, M. Hallek, A. Ultsch, C. M. Wendtner, *Leukemia* **2008**, *22*, 585–585.
- [9] a) S. K. Mamidyala, M. G. Finn, *Chem. Soc. Rev.* **2010**, *39*, 1252–1261; b) E. M. Sletten, C. R. Bertozzi, *Angew. Chem.* **2009**, *121*, 7108–7133; *Angew. Chem. Int. Ed.* **2009**, *48*, 6974–6998; c) M. Meldal, C. W. Tornøe, *Chem. Rev.* **2008**, *108*, 2952–3015; d) K. A. Kalesh, H. Shi, J. Ge, S. Q. Yao, *Org. Biomol. Chem.* **2010**, *8*, 1749–1762.
- [10] a) G. Ma, M. Zancanella, Y. Oyola, R. D. Richardson, J. W. Smith, D. Romo, *Org. Lett.* **2006**, *8*, 4497–4500; b) R. D. Richardson, G. Ma, Y. Oyola, M. Zancanella, L. M. Knowel, P. Cieplak, D. Romo, J. W. Smith, *J. Med. Chem.* **2008**, *51*, 5285–5296.
- [11] a) W. Hillaert, M. Verdoes, B. I. Florea, N. Saragliadis, K. L. L. Habets, J. Kuiper, S. Van Calenbergh, F. Ossendorp, G. A. van der Marel, C. Driessen, H. S. Overkleeft, *Angew. Chem.* **2009**, *121*, 1657–1660; *Angew. Chem. Int. Ed.* **2009**, *48*, 1629–1632; b) M. P. Pereira, S. O. Kelley, *J. Am. Chem. Soc.* **2011**, *133*, 3260–3263; c) Y. Loh, H. Shi, M. Hu, S. Q. Yao, *Chem. Commun.* **2010**, *46*, 8407–8409; d) D. Srikun, A. E. Albers, C. I. Nam, A. T. Iavaron, C. J. Chang, *J. Am. Chem. Soc.* **2010**, *132*, 4455–4465.
- [12] a) A. Keppler, S. Gendreizig, T. Gronemeyer, H. Pick, H. Vogel, K. Johnsson, *Nat. Biotechnol.* **2003**, *21*, 86–89; b) A. Juillerat, T. Gronemeyer, A. Keppler, S. Gendreizig, H. Pick, H. Vogel, K. Johnsson, *Chem. Biol.* **2003**, *10*, 313–317; c) A. Keppler, M. Kindermann, S. Gendreizig, H. Pick, H. Vogel, K. Johnsson, *Methods* **2004**, *32*, 437–444; d) A. Gautier, A. Juillerat, C. Heinis, I. R. Correa, M. Kindermann, F. Beaufils, K. Johnsson, *Chem. Biol.* **2008**, *15*, 128–136.
- [13] Y.-C. Teo, K.-T. Tan, T.-P. Loh, *Chem. Commun.* **2005**, 1318–1320.
- [14] a) S. Wong, J. McLaughlin, D. Cheng, C. Zhang, K. M. Shokat, O. N. Witte, *Proc. Natl. Acad. Sci. USA* **2004**, *101*, 17456–17461; b) C. Kung, D. M. Kenski, S. H. Dickerson, R. W. Howson, L. F. Kuyper, H. D. Madhani, K. M. Shokat, *Proc. Natl. Acad. Sci. USA* **2005**, *102*, 3587–3592.
- [15] a) S. H. Verhelst, M. Fonovic, M. Bogyo, *Angew. Chem.* **2007**, *119*, 1306–1308; *Angew. Chem. Int. Ed.* **2007**, *46*, 1284–1286; b) Y. Y. Yang, J. M. Ascano, H. C. Hang, *J. Am. Chem. Soc.* **2010**, *132*, 3640–3641; c) J. Szychowski, A. Mahdavi, J. J. L. Hodas, J. D. Bagert, J. T. Ngo, P. Landgraf, D. C. Dieterich, E. M. Schuman, D. A. Tirrell, *J. Am. Chem. Soc.* **2010**, *132*, 18351–18360.
- [16] Z. Ma, C. Chu, D. J. Cheng, *J. Lipid Res.* **2009**, *50*, 2131–2135.
- [17] C. A. Brautigam, J. L. Chuang, D. R. Tomchick, M. Machius, D. T. Chuang, *J. Mol. Biol.* **2005**, *350*, 543–552.
- [18] J. L. Periago, M. L. Pita, M. A. Sanchez del Castillo, G. Caamaño, M. D. Suárez, *Lipids* **1989**, *24*, 383–388.
- [19] G. B. Kudolo, M. J. Harper, *J. Lipid Mediators Cell Signalling* **1995**, *11*, 145–158.
- [20] R. Sundaramoorthy, E. Micossi, M. S. Alphey, V. Germain, J. H. Bryce, S. M. Smith, G. A. Leonard, W. N. Hunter, *J. Mol. Biol.* **2006**, *359*, 347–357.
- [21] a) K. Moreau, E. Dizin, H. Ray, C. Luquain, E. Lefai, F. Foufelle, M. Billaud, G. M. Lenoir, N. D. Venezia, *J. Biol. Chem.* **2005**, *281*, 3172–3181; b) S. Y. Bu, M. T. Mashek, D. G. Mashek, *J. Biol. Chem.* **2009**, *284*, 30474–30483.
- [22] a) J. Y. Lu, L. A. Verkruyse, S. L. Hofmann, *Proc. Natl. Acad. Sci. USA* **1996**, *93*, 10046–10050; b) A. Dahlqvist, U. Ståhl, M. Lenman, A. Banas, M. Lee, L. Sandager, H. Ronne, S. Stymne, *Proc. Natl. Acad. Sci. USA* **2000**, *97*, 6487–6492.
- [23] a) S. E. Ong, M. Mann, *Nat. Chem. Biol.* **2005**, *1*, 252–262; b) M. Bantscheff, M. Schirle, G. Sweetman, J. Rick, B. Kuster, *Anal. Bioanal. Chem.* **2007**, *389*, 1017–1031.
- [24] a) W. Zhu, J. W. Smith, C. M. Huang, *J. Biomed. Biotechnol.* **2010**, *2010*, 840518; b) H. Liu, R. G. Sadygov, J. R. Yates 3rd, *Anal. Chem.* **2004**, *76*, 4193–4201; c) Y. Ishihama, Y. Oda, T. Tabata, T. Sato, T. Nagasu, J. Rappsilber, M. Mann, *Mol. Cell. Proteomics* **2005**, *4*, 1265–1272; d) K. Shinoda, M. Tomita, Y. Ishihama, *Bioinformatics* **2010**, *26*, 576–577.
- [25] a) P. J. R. Goulder, D. I. Watkins, *Nat. Rev. Immunol.* **2008**, *8*, 619–630; b) Y. Kawashima, K. Pfafferott, J. Frater, P. Matthews, R. Payne, M. Addo, H. Gatanaga, M. Fujiwara, A. Hachiya, H. Koizumi, N. Kuse, S. Oka, A. Duda, A. Prendergast, H. Crawford, A. Leslie, Z. Brumme, C. Brumme, T. Allen, C. Brander, R. Kaslow, J.

- Tang, E. Hunter, S. Allen, J. Mulenga, S. Branch, T. Roach, M. John, S. Mallal, A. Ogwu, R. Shapiro, J. G. Prado, S. Fidler, J. Weber, O. G. Pybus, P. Klenerman, T. Ndung'u, R. Phillips, D. Heckerman, P. R. Harrigan, B. D. Walker, M. Takiguchi, P. Goulder, *Nature* **2009**, *458*, 641–645; c) P. Kiepiela, A. J. Leslie, I. Honeyborne, D. Ramduth, C. Thobakgale, S. Chetty, P. Rathnavalu, C. Moore, K. J. Pfafferott, L. Hilton, P. Zimbwa, S. Moore, T. Allen, C. Brander, M. M. Addo, M. Altfeld, I. James, S. Mallal, M. Bunce, L. D. Barber, J. Szinger, C. Day, P. Klenerman, J. Mullins, B. Korber, H. M. Coovadia, B. D. Walker, P. J. Goulder, *Nature* **2004**, *432*, 769–775.
- [26] a) S. R. Neves, P. T. Ram, R. Iyengar, *Science* **2002**, *296*, 1636–1639; b) J. C. Migeon, S. L. Thomas, N. M. Nathanson, *J. Biol. Chem.* **1994**, *269*, 29146–29152; c) J. F. Foley, S. P. Singh, M. Cantu, L. Chen, H. H. Zhang, J. M. Farber, *J. Biol. Chem.* **2010**, *285*, 35537–35550.
- [27] J. Diekmann, E. Adamopoulou, O. Beck, G. Rauser, S. Lurati, S. Tenzer, H. Einsele, H. G. Rammensee, H. Schild, M. S. Topp, *J. Immunol.* **2009**, *183*, 1587–1597.
- [28] N. de La Iglesia, G. Konopka, S. V. Puram, J. A. Chan, R. M. Bachoo, M. J. You, D. E. Levy, R. A. Depinho, A. Bonni, *Genes Dev.* **2008**, *22*, 449–462.
- [29] S. Jaisson, M. Veiga-da-Cunha, E. Van Schaftingen, *Biochimie* **2009**, *91*, 1066–1071.
- [30] a) L. Rajendran, H. J. Knölker, K. Simons, *Nat. Rev. Drug Discovery* **2010**, *9*, 29–42; b) L. Rajendran, A. Schneider, G. Schlechtingen, S. Weidlich, J. Ries, T. Braxmeier, P. Schwille, J. B. Schulz, C. Schroeder, M. Simons, G. Jennings, H. J. Knolker, K. Simons, *Science* **2008**, *320*, 520–523.
- [31] a) A. Keppler, H. Pick, C. Arrivoli, H. Vogel, K. Johnsson, *Proc. Natl. Acad. Sci. USA* **2004**, *101*, 9955–9959; b) E. Tomat, E. M. Nolan, J. Jaworski, S. J. Lippard, *J. Am. Chem. Soc.* **2008**, *130*, 15776–15777; c) M. Bannwarth, I. R. Correa, M. Sztretye, S. Pouvreau, C. Fellay, A. Aebischer, L. Royer, E. Rios, K. Johnsson, *ACS Chem. Biol.* **2009**, *4*, 179–190; d) M. Kamiya, K. Johnsson, *Anal. Chem.* **2010**, *82*, 6472–6479.
- [32] AGT is endogenously expressed in most mammalian cell lines. Its presence will lead to interference with our assay and high background conjugation/labeling.
- [33] a) S. W. Taylor, E. Fahy, S. S. Ghosh, *Trends Biotechnol.* **2003**, *21*, 82–88; b) A. Y. Andreyev, Z. Shen, Z. Guan, A. Ryan, E. Fahy, S. Subramaniam, C. R. Raetz, S. Briggs, E. A. Dennis, *Mol. Cell. Proteomics* **2010**, *9*, 388–402.
- [34] a) C. S. Gan, T. Guo, H. Zhang, S. K. Lim, S. K. Sze, *J. Proteome Res.* **2008**, *7*, 4869–4877; b) P. Hao, T. Guo, X. Li, S. S. Adav, J. Yang, M. Wei, S. K. Sze, *J. Proteome Res.* **2010**, *9*, 3520–3526.

Received: March 25, 2011
Published online: July 8, 2011